

Electronic Supplementary Information (ESI) for

Symmetrically Substituted Siloles on Their 2,5-Positions with Electron-Accepting and Donating Moieties: Facile Synthesis, Aggregation-Enhanced Emission, Solvatochromism, and Device Application

Ju Mei,^a Jian Wang,^a Jing Zhi Sun,^a Hui Zhao,^a Wangzhang Yuan,^b Chunmei Deng,^b Shuming Chen,^c Herman H. Y. Sung,^b Ping Lu,^d Anjun Qin,^{*a} Hoi Sing Kwok,^c Yuguang Ma,^d Ian D. Williams,^b and Ben Zhong Tang^{*a,b}

^a MOE Key Laboratory of Macromolecular Synthesis and Functionalization, Department of Polymer Science and Engineering, Zhejiang University, Hangzhou 310027, China. E-mail: qinaj@zju.edu.cn, tangbenz@ust.hk

^b Department of Chemistry, The Hong Kong University of Science & Technology (HKUST), Clear Water Bay, Kowloon, Hong Kong, China

^c Center for Display Research, HKUST, Clear Water Bay, Kowloon, Hong Kong, China

^d State Key Lab Supramolecular Structure & Materials, Jilin University, Changchun 130012, PR China

Table of Contents

Figure S1. ¹ H NMR spectra of 2-(4-bromophenyl)-1,3-dioxolane in CDCl ₃ .	(2)
Figure S2. ¹³ C NMR spectra of 2-(4-bromophenyl)-1,3-dioxolane in CDCl ₃ .	(2)
Figure S3. ¹ H NMR spectra of DMTPS-ALD in CDCl ₃ .	(2)
Figure S4. ¹³ C NMR spectra of DMTPS-ALD in CDCl ₃ .	(3)
Figure S5. ¹ H NMR spectra of DMTPS-DCV in CDCl ₃ .	(3)
Figure S6. ¹³ C NMR spectra of DMTPS-DCV in CDCl ₃ .	(3)
Figure S7. ¹ H NMR spectra of DMTPS-DPA in CDCl ₃ .	(4)
Figure S8. ¹³ C NMR spectra of DMTPS-DPA in CDCl ₃ .	(4)
Figure S9. MALDI-TOF mass spectrum of DMTPS-DCV.	(4)
Figure S10. DSC graphs of silole derivatives.	(5)
Figure S11. PL spectra of DMTPS-ALD (a) and DMTPS-DPA (b) in THF/water mixtures.	(5)
Figure S12. Absorption spectra of silole derivatives in THF/water mixtures.	(5)
Figure S13. PL spectra of silole derivatives in (a) THF solution and (b) film states.	(6)
Figure S14. Photographs of silole derivatives under ambient light and UV light.	(6)
Figure S15. Molecular structures and torsion angles of silole derivatives.	(6)
Figure S16. Representative intramolecular C-H···π interactions of silole derivatives.	(7)
Figure S17. Representative intermolecular C-H···π interactions of silole derivatives.	(7)
Figure S18. Normalized absorption spectra of silole in solvents with varying polarity.	(8)
Figure S19. Plots between emission wavelength and empirical parameters solvent polarity.	(8)
Figure S20. The cyclic voltammograms of silole in CH ₂ Cl ₂ / 0.1M [ⁿ Bu ₄ N] ⁺ [PF ₆] ⁻ at 50 mV s ⁻¹ .	(8)
Table S1. Crystallographic Data and Structure Refinement for DMTPS-ALD.	(9)
Table S2. Crystallographic Data and Structure Refinement for DMTPS-DPA.	(10)

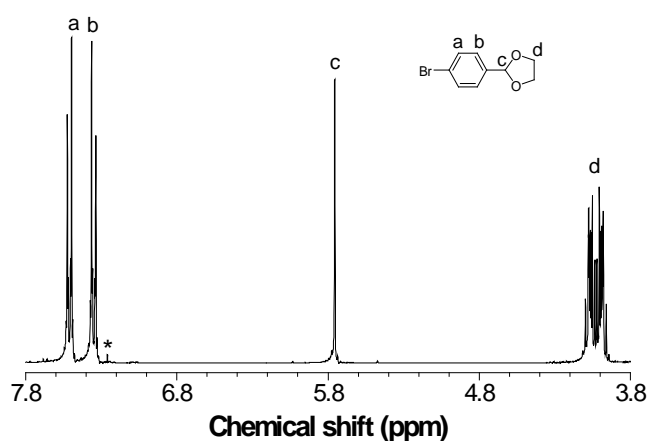


Figure S1. ^1H NMR spectrum of **4** in CDCl_3 . The solvent peak is marked with asterisk.

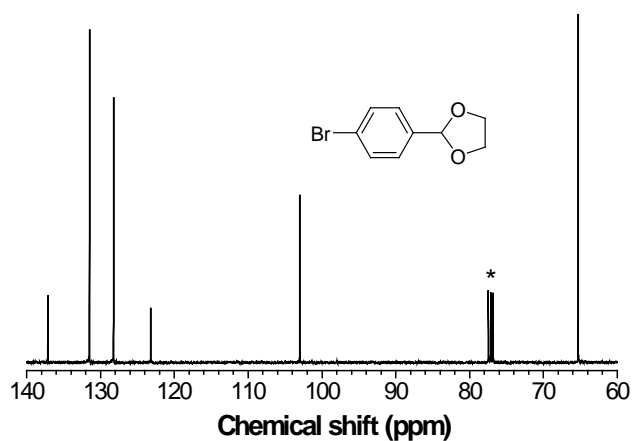


Figure S2. ^{13}C NMR spectrum of **4** in CDCl_3 . The solvent peak is marked with asterisk.

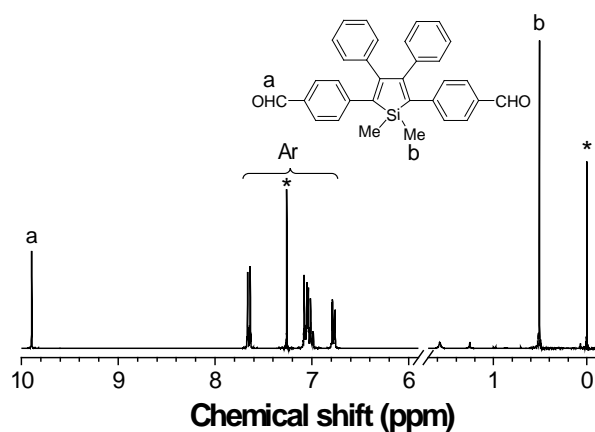


Figure S3. ^1H NMR spectrum of DMTPS-ALD in CDCl_3 . The solvent peaks are marked with asterisks.

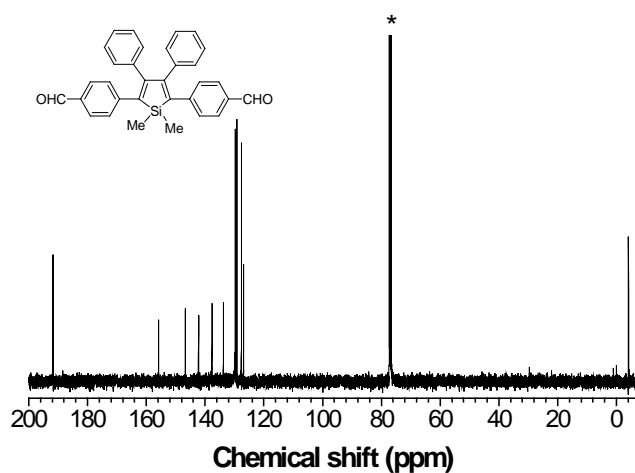


Figure S4. ^{13}C NMR spectrum of DMTPS-ALD in CDCl_3 . The solvent peak is marked with asterisk.

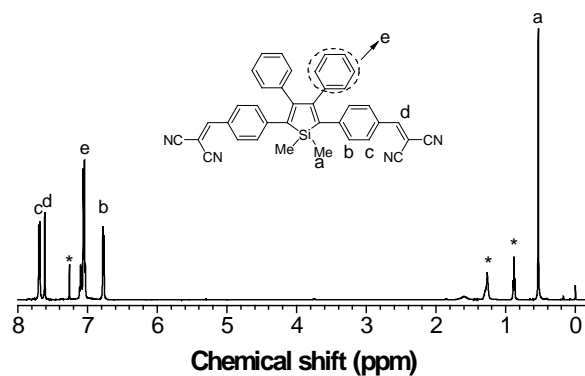


Figure S5. ^1H NMR spectrum of DMTPS-DCV in CDCl_3 . The solvent peaks are marked with asterisks.

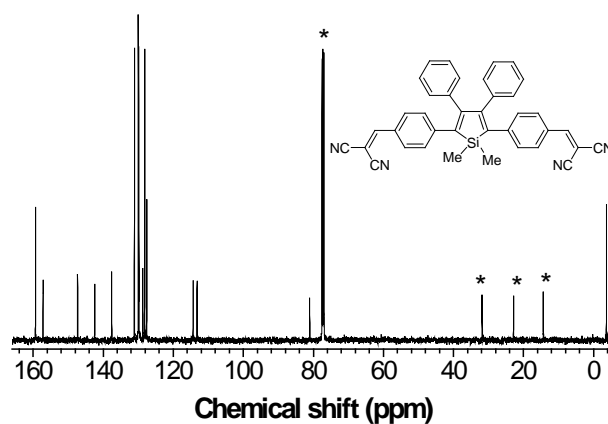


Figure S6. ^{13}C NMR spectrum of DMTPS-DCV in CDCl_3 . The solvent peaks are marked with asterisks.

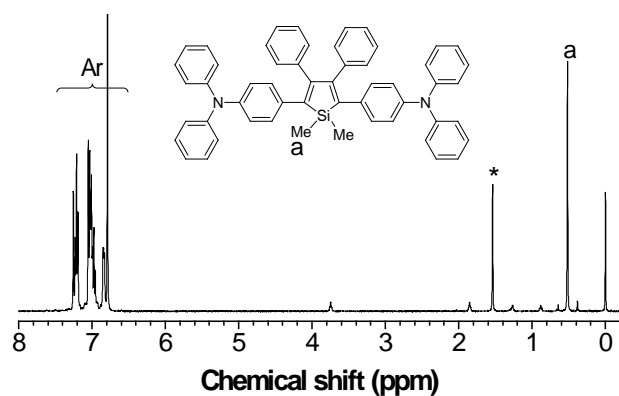


Figure S7. ^1H NMR spectrum of DMTPS-DPA in CDCl_3 . The solvent peaks are marked with asterisks.

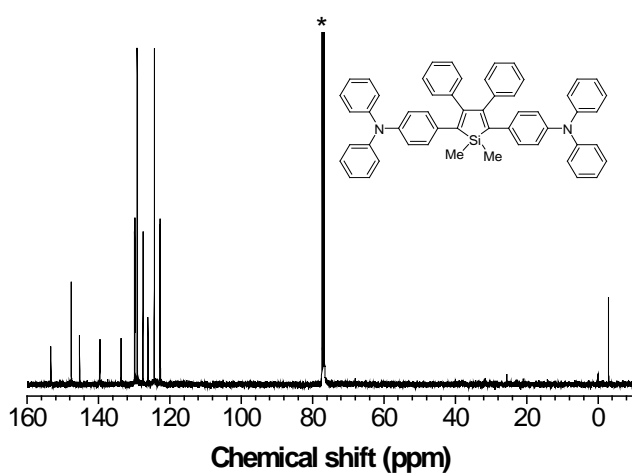


Figure S8. ^{13}C NMR spectrum of DMTPS-DPA in CDCl_3 . The solvent peak is marked with asterisk.

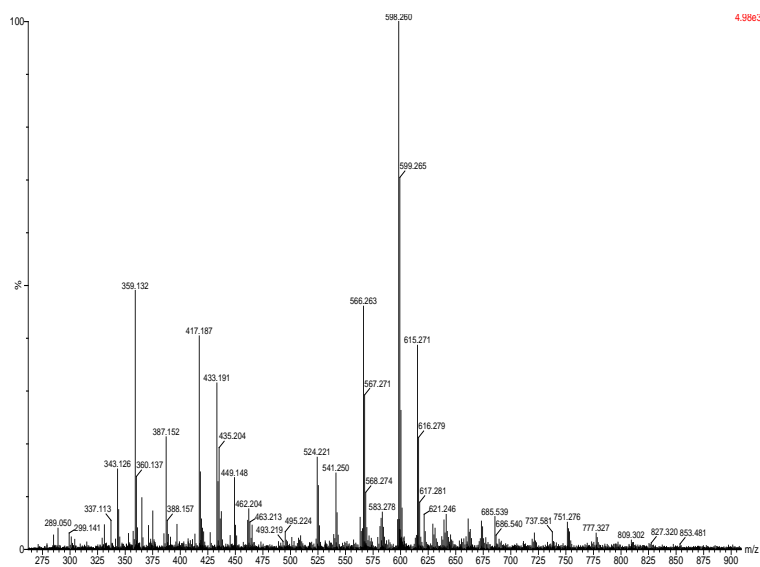


Figure S9. High resolution mass (HRMS) spectrum of DMTPS-DCV.

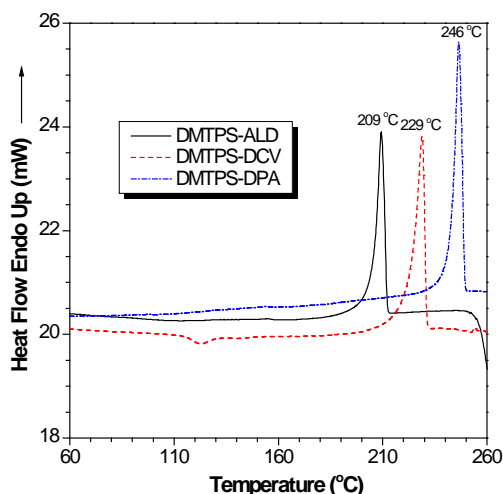


Figure S10. DSC graphs of silole derivatives. Heating rate: 10 °C/min, atmosphere: N₂.

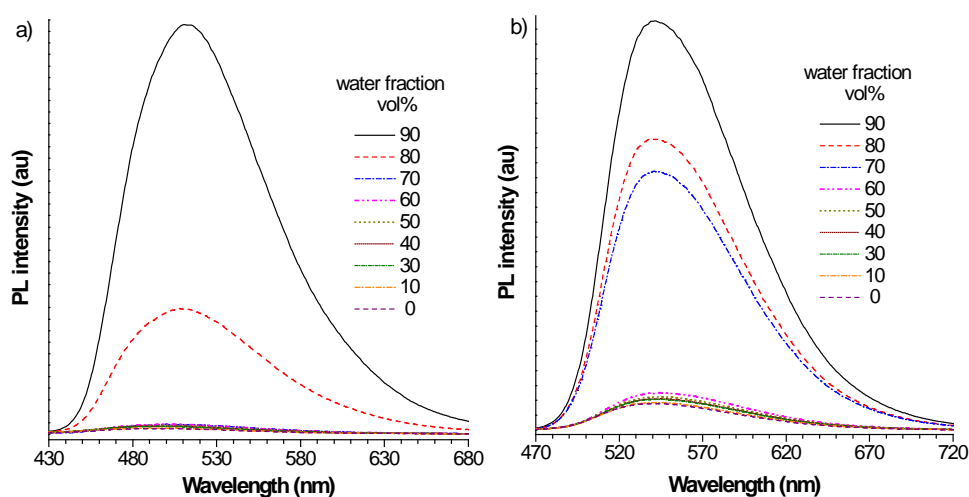


Figure S11. PL spectra of DMTPS-ALD (a) and DMTPS-DPA (b) in THF/water mixtures with different water fraction at room temperature. $\lambda_{\text{ex}} = 377$ and 422 nm, concentration = 20 and 10 μM , respectively.

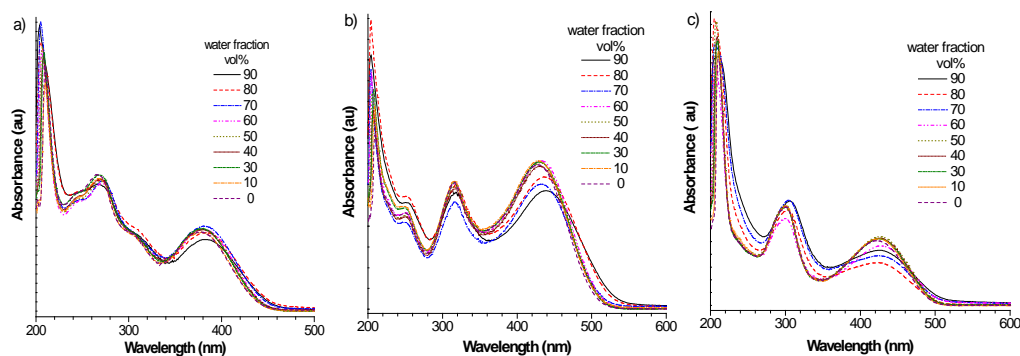


Figure S12. Absorption spectra of (a) DMTPS-ALD, concentration (c) = 20 μM , (b) DMTPS-DCV, c = 10 μM , and (c) DMTPS-DPA, c = 10 μM in THF/water mixtures with different water fraction at room temperature.

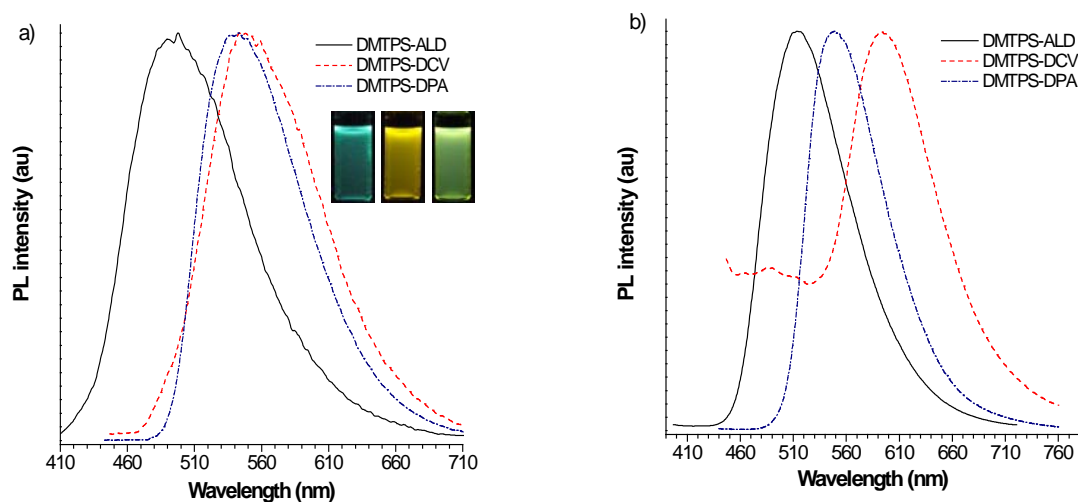


Figure S13. PL spectra of silole derivatives in (a) THF solution (concentration: 2×10^{-4} M) and (b) film states, respectively. The inset in panel (a) is the corresponding photographs of their solutions taken under UV lamp (365 nm).

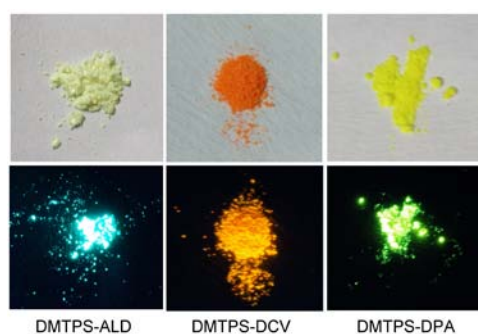


Figure S14. Photographs of silole derivatives under ambient light (top panel) and UV light (bottom panel).

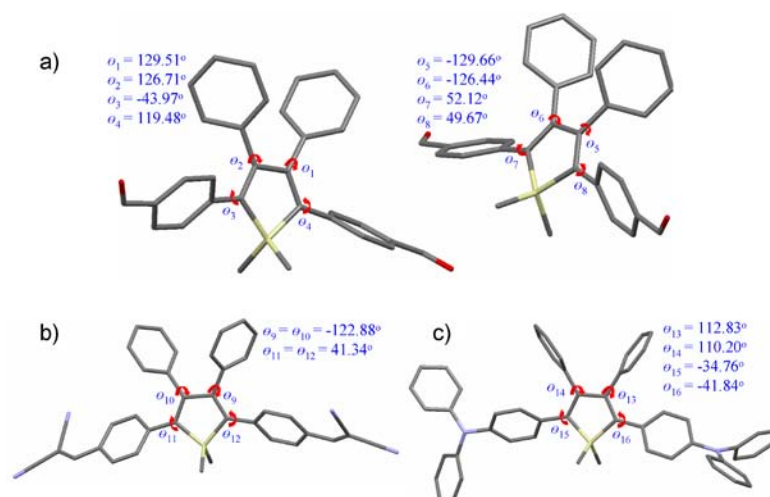


Figure S15. Molecular structures and torsion angles of (a) DMTPS-ALD, (b) DMTPS-DCV and (c) DMTPS-DPA. The atoms are represented as sticks in all panels. Si, N, O, and C atoms are in light yellow, purple, red, and grey, respectively. All the H atoms are omitted for clarity.

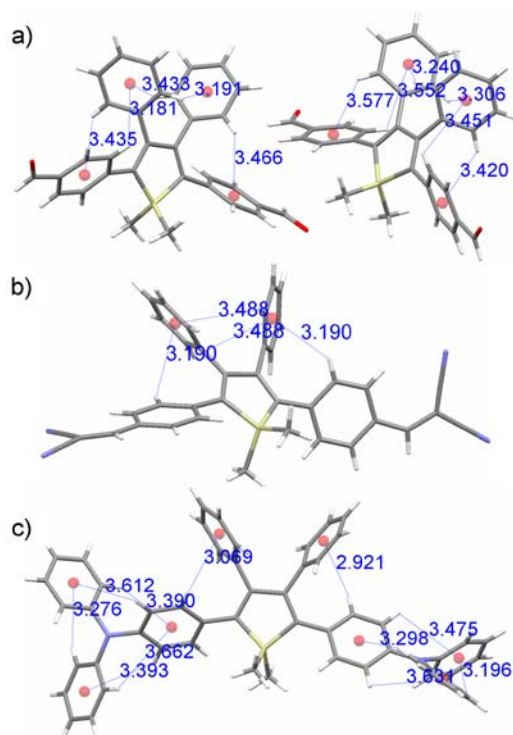


Figure S16. Representative intramolecular C-H... π interactions with indicated distances (Å) of (a) DMTPS-ALD, (b) DMTPS-DCV and (c) DMTPS-DPA.

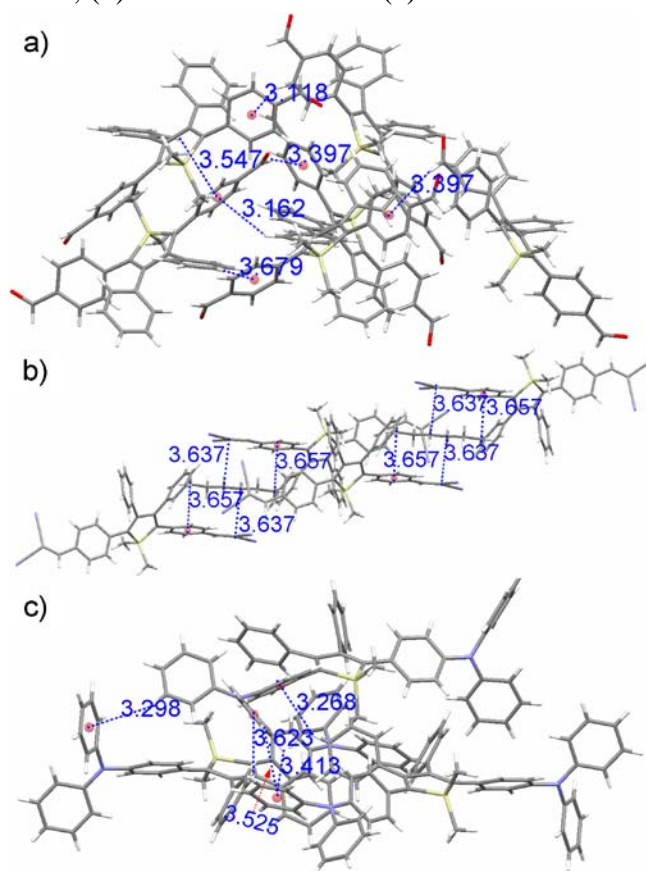


Figure S17. Representative intermolecular C-H... π interactions with indicative distances (Å) of (a) DMTPS-ALD, (b) DMTPS-DCV and (c) DMTPS-DPA. Panel (b) also shows the J-aggregation interaction of DMTPS-DCV.

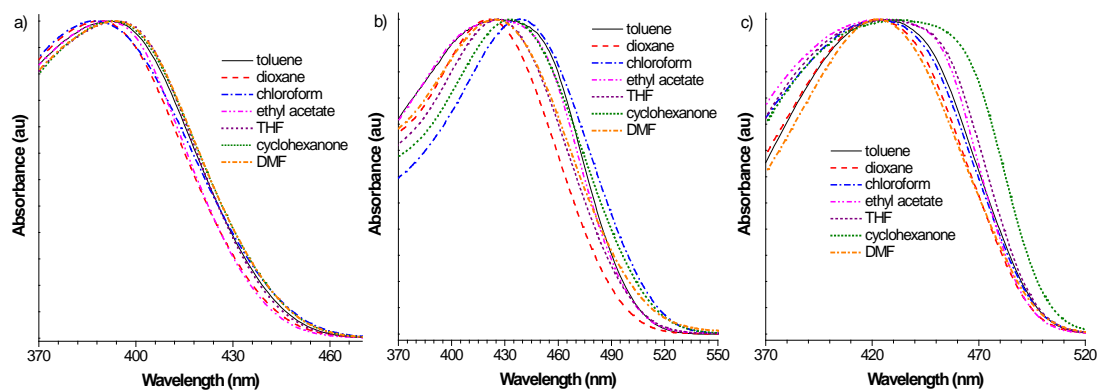


Figure S18. Normalized absorption spectra of DMTPS-ALD (a), DMTPS-DCV (b), and DMTPS-DPA (c) in solvents with varying polarity. Concentration: 2×10^{-4} M.

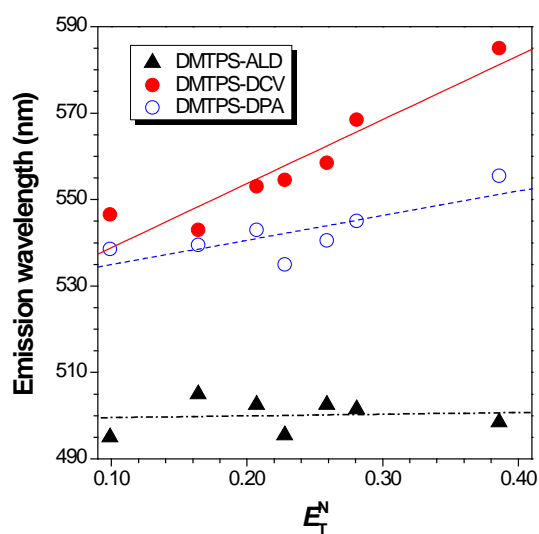


Figure S19. The dependency of the emission wavelengths of silole derivatives on the empirical parameters (E_T^N) of solvent polarity. Where,

$$E_T^N = \frac{E_T(\text{solvent}) - E_T(\text{TMS})}{E_T(\text{water}) - E_T(\text{TMS})} = \frac{E_T(\text{solvent}) - 30.7}{32.4} \quad (\text{TMS} = \text{tetramethylsilane})$$

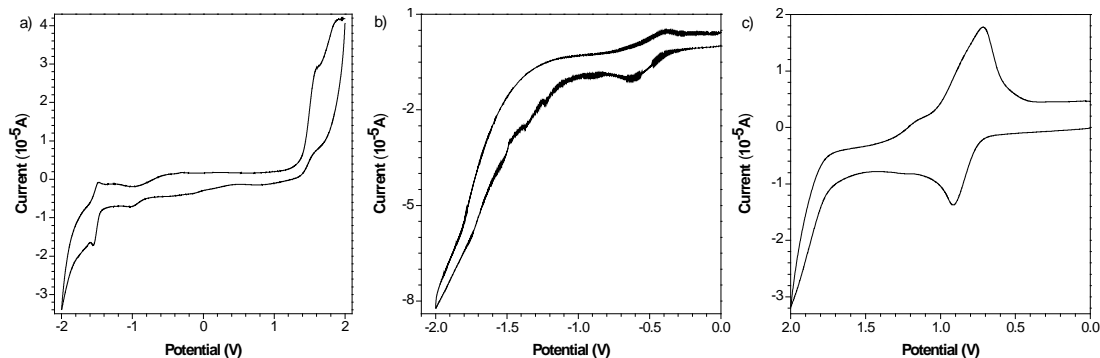


Figure S20. The cyclic voltammograms of DMTPS-ALD (a), DMTPS-DCV (b), and DMTPS-DPA (c) in $\text{CH}_2\text{Cl}_2/0.1\text{M} [\text{nBu}_4\text{N}]^+[\text{PF}_6]^-$ at a rate of 50 mV s^{-1} .

Table S1. Crystal Data and Structure Refinement for DMTPS-ALD

Empirical formula	C ₃₂ H ₂₆ O ₂ Si
Formula weight	470.62
Temperature	173(2) K
Wavelength	1.54178 Å
Crystal system	Orthorhombic
Space group	Pbca
Unit cell dimensions	a = 21.7477(9) Å $\alpha = 90^\circ$ b = 13.4689(6) Å $\beta = 90^\circ$ c = 35.5044(11) Å $\gamma = 90^\circ$
Volume	10399.9(7) Å ³
Z	16
Density (calculated)	1.202 mg m ⁻³
Absorption coefficient	0.996 mm ⁻¹
F(000)	3968
Crystal size	0.30 × 0.07 × 0.06 mm ³
Theta range for data collection	2.49 to 67.49°.
Index ranges	-25 ≤ h ≤ 23, -14 ≤ k ≤ 16 -42 ≤ l ≤ 31
Reflections collected	28501
Independent reflections	9219 [R(int) = 0.0610]
Completeness to theta = 66.50°	98.4 %
Absorption correction	Semi-empirical from equivalents
Max. and min. transmission	1.00 and 0.81
Refinement method	Full-matrix least-squares on F ²
Data / restraints / parameters	9219 / 0 / 635
Goodness-of-fit on F ²	1.015
Final R indices [I > 2σ(I)]	R1 = 0.0456, wR2 = 0.0770
R indices (all data)	R1 = 0.0958, wR2 = 0.0847
Largest diff. peak and hole	0.485 and -0.283 e.Å ⁻³

Table S2. Crystal Data and Structure Refinement for DMTPS-DPA.

Empirical formula	C ₅₄ H ₄₄ N ₂ Si
Formula weight	749.00
Temperature	133(2) K
Wavelength	1.5418 Å
Crystal system	Monoclinic
Space group	P2(1)/c
Unit cell dimensions	a = 20.3587(4) Å α = 90° b = 11.0369(3) Å β = 93.111(2)° c = 18.2729(8) Å γ = 90°
Volume	4099.8(2) Å ³
Z	4
Density (calculated)	1.213 mg m ⁻³
Absorption coefficient	0.800 mm ⁻¹
F(000)	1584
Crystal size	0.40 × 0.37 × 0.07 mm ³
Theta range for data collection	4.35 to 67.47°.
Index ranges	-15 ≤ h ≤ 24 -13 ≤ k ≤ 10 -21 ≤ l ≤ 21
Reflections collected	13752
Independent reflections	7105 [R(int) = 0.0273]
Completeness to theta = 66.50°	96.3 %
Absorption correction	Semi-empirical from equivalents
Max. and min. transmission	1.00 and 0.66
Refinement method	Full-matrix least-squares on F ²
Data / restraints / parameters	7105 / 0 / 516
Goodness-of-fit on F ²	1.020
Final R indices [I > 2σ(I)]	R1 = 0.0371, wR2 = 0.0902
R indices (all data)	R1 = 0.0485, wR2 = 0.0933
Largest diff. peak and hole	0.288 and -0.283 e.Å ⁻³